NANO LETTERS

2009
Vol. 9, No. 9
3365-3369

Direct Imaging of Soft−Hard Interfaces Enabled by Graphene

Zonghoon Lee,*,† Ki-Joon Jeon,*,‡ Albert Dato,*,§ Rolf Erni,† Thomas J. Richardson,‡ Michael Frenklach,|| and Velimir Radmilovic†

National Center for Electron Microscopy, Environmental Energy Technologies Division, Lawrence Berkeley National Laboratory, Berkeley, California 94720, and Applied Science and Technology Graduate Group, Department of Mechanical Engineering, University of California, Berkeley, California 94720

Received May 26, 2009; Revised Manuscript Received June 23, 2009

Downloaded by U OF CALIFORNIA BERKELEY on September 22, 2009 | http://pubs.acs.org
Publication Date (Web): July 10, 2009 | doi: 10.1021/nl901664k

ABSTRACT

Direct imaging of surface molecules and the interfaces between soft and hard materials on functionalized nanoparticles is a great challenge using modern microscopy techniques. We show that graphene, a single atomic layer of sp^2-bonded carbon atoms, can be employed as an ultrathin support film that enables direct imaging of molecular layers and interfaces in both conventional and atomic-resolution transmission electron microscopy. An atomic-resolution imaging study of the capping layers and interfaces of citrate-stabilized gold nanoparticles is used to demonstrate this novel capability. Our findings reveal the unique potential of graphene as an ideal support film for atomic-resolution transmission electron microscopy of hard and soft nanomaterials.

The interfaces between soft and hard materials (soft−hard interfaces) have attracted great interest throughout the scientific community. For example, nanoparticles coated with molecular layers can self-assemble into novel structures[1−12] that are envisioned for use in sensors, photonics, and electronics.[5] The nature of these molecular coatings, such as chemical "patchiness",[3−5] can dictate self-assembly, and thus more detailed analysis of these soft materials is needed. However, surface molecules and their interfaces with nanoparticles cannot be clearly imaged at the atomic-scale using current microscopy techniques.

It has been shown that transmission electron microscope (TEM) imaging of functionalized nanoparticles is feasible,[6−9] but in even the most recent study, it was not possible to observe molecular surface layers and soft−hard interfaces at the atomic level.[13] Aberration-corrected TEMs can attain subangstrom resolution at low accelerating voltages.[14,15] Such microscopes can produce atomic-resolution images of nanomaterials without rapid electron beam damage that occurs at higher accelerating voltages. However, conventional TEM support films, such as ultrathin amorphous carbon, which still has a thickness of 2−3 nm, limit the capabilities of these advanced microscopes because they contribute to overall electron scattering and diminish the contrast of low-atomic-number specimens.[14] TEM imaging of molecular coatings therefore requires improved support materials showing lower dynamical interference with an imaging object.

Graphene has been proposed as an ideal TEM support.[14,15] It is atomically thin, chemically inert, consists of light atoms, and possesses a highly ordered structure. Additionally, the material is electrically[14] and thermally conductive,[16] as well as structurally stable.[17] These remarkable properties have enabled the detection of hydrogen atoms and carbon adsorbates on a graphene sheet in a conventional TEM.[14] As demonstrated here, the TEM imaging of molecular layers and interfaces between hard and soft materials can be achieved using graphene.

The graphene membranes used in the present studies were synthesized using the substrate-free gas-phase method.[18] Graphene sheets were sonicated in ethanol to form a homogeneous suspension. Citrate-capped gold nanoparticles (BBI Inc., 10 nm average diameter) were introduced into the suspension, which was then shaken by hand for 30 s to form a dispersion of nanoparticles and graphene. A drop of the suspension was deposited onto a Cu TEM grid with a lacey carbon support, which was air-dried prior to TEM characterization. A typical low-magnification image, obtained using a conventional TEM (Zeiss Libra 200 FEG, 200 kV accelerating voltage), revealed that the nanoparticles were exceptionally well-dispersed on the graphene supports, which were typically folded and overlapping (Figure 1). Single-

* To whom correspondence should be addressed. E-mail: (Z.L.) zhlee@lbl.gov; (K.-J.J.) kjjeon@lbl.gov; (A.D.) amdato@newton.berkeley.edu.
† National Center for Electron Microscopy, Lawrence Berkeley National Laboratory.
‡ Environmental Energy Technologies Division, Lawrence Berkeley National Laboratory.
§ Applied Science and Technology Graduate Group, University of California.
|| Department of Mechanical Engineering, University of California.

10.1021/nl901664k CCC: $40.75 © 2009 American Chemical Society
Published on Web 07/10/2009

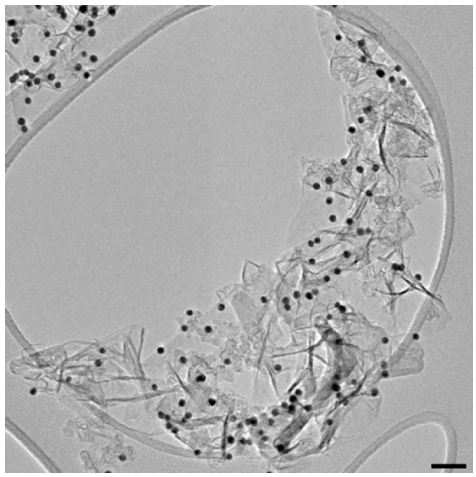

Figure 1. A low-magnification TEM image of gold nanoparticles coated with citrate on synthesized graphene sheets. Scale bar represents 50 nm.

layer, bilayer, and few-layer sheets were created during the synthesis process,[18] and nanoparticles were observed on each of these species during experiments. TEM characterization at higher magnifications was carried out on nanoparticles that were located near the edges and planar areas of graphene sheets (Figure 2a). Sheet edges were visible at a defocused condition of −150 nm, and an intensity profile (Figure 2b) taken along the dashed line in the image showed bright contrast contributed by the edges of the nanoparticle, graphene support, and the amorphous lacey carbon film. Despite its visibility, the graphene membrane exhibited a much lower contrast variation than the amorphous support. The graphene sheet became nearly indistinguishable from the vacuum in an image of the same region that was taken at a focused condition (Figure 2c). The intensity profile (Figure 2d) showed that the vacuum and graphene had similar intensities, while the contrast of the nanoparticle and amorphous support were still clearly observable. The noticeable blurred and undulating features around the nanoparticle (inset of Figure 2c) indicate the presence of the citrate coating, which was detected because the graphene support was nearly electron-invisible. Although the interface between a nanoparticle and its capping layer was detectable in this

Downloaded by U OF CALIFORNIA BERKELEY on September 22, 2009 | http://pubs.acs.org
Publication Date (Web): July 10, 2009 | doi: 10.1021/nl901664k

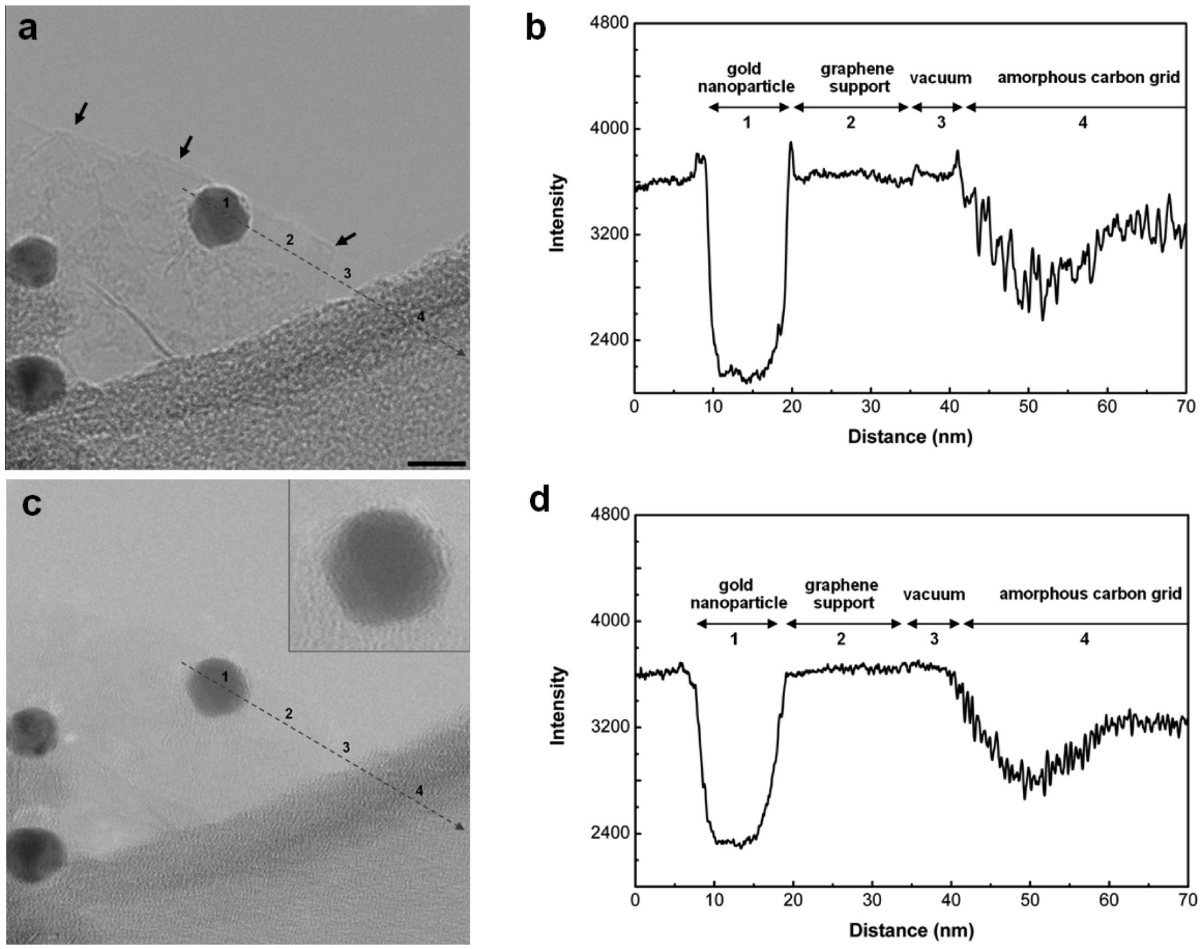

Figure 2. Graphene an invisible support in conventional TEM. (a) A high-magnification defocused image of a nanoparticle near the edge of a graphene sheet. The arrows indicate the edges of the sheet. The image was obtained in a TEM with a spherical aberration of 2.2 mm. The numbers 1, 2, 3, and 4 on the dashed line indicate the regions corresponding to the nanoparticle, graphene sheet, vacuum, and amorphous carbon support, respectively. Scale bar represents 10 nm. (b) An intensity profile obtained along the dashed line in the defocused image. The intensity spikes are due to the edge contrast of the nanoparticle, graphene sheet, and amorphous carbon. (c) The same image taken at a focused condition. (Inset) A gold nanoparticle coated with citrate molecules. (d) The corresponding intensity profile of the focused image. The graphene support and the vacuum have a similar profile.

Downloaded by U OF CALIFORNIA BERKELEY on September 22, 2009 | http://pubs.acs.org
Publication Date (Web): July 10, 2009 | doi: 10.1021/nl901664k

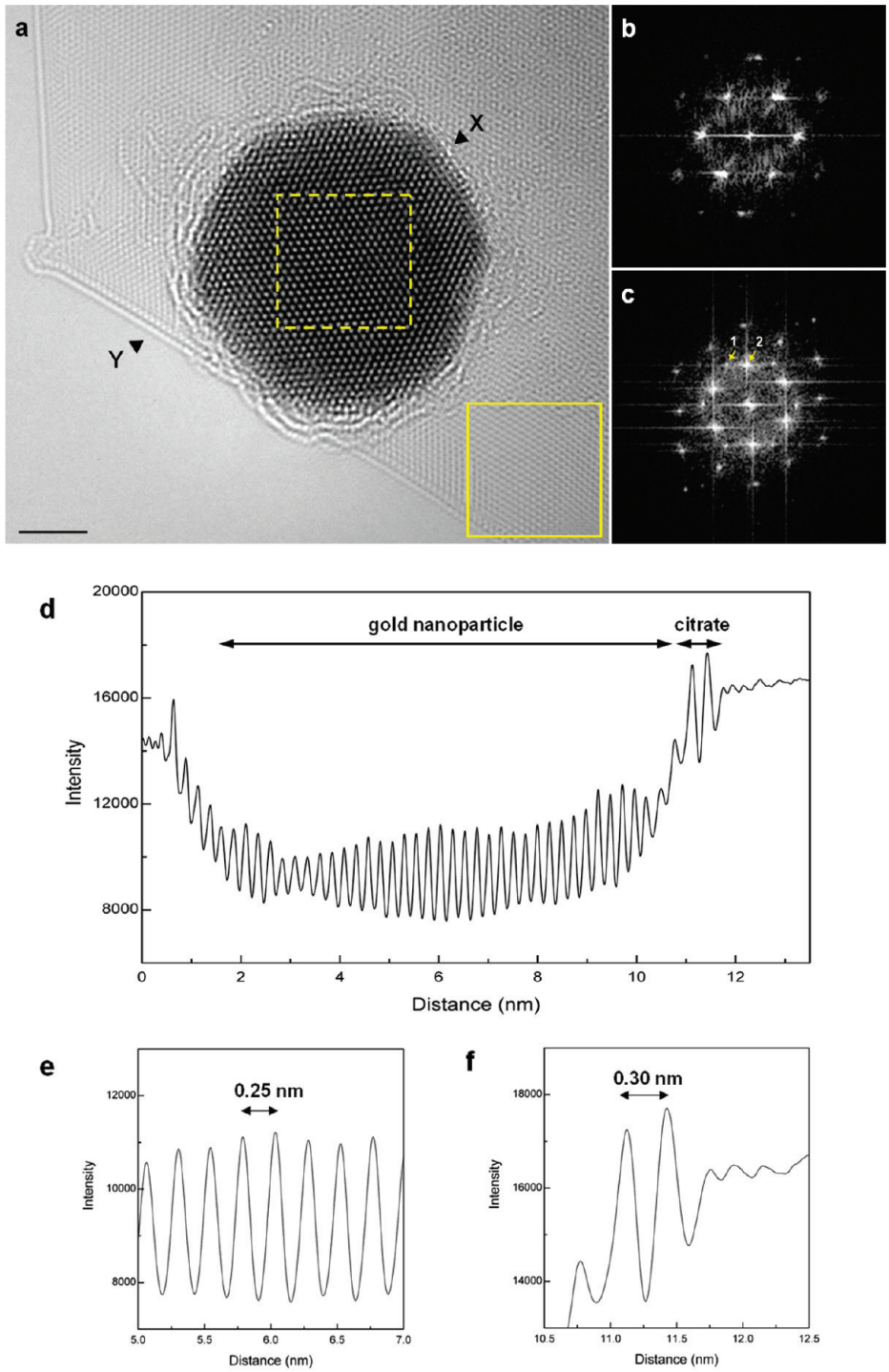

Figure 3. Atomic-resolution imaging of the gold-citrate interface. (a) An atomic-resolution image of a gold nanoparticle and its surrounding citrate capping agent. Scale bar represents 2 nm. (b) Digital diffractogram of the graphene membrane taken from the region indicated by the solid box in the TEM image. (c) Digital diffractogram taken from the region indicated by the dashed box. Arrows 1 and 2 note reflections corresponding to graphene and gold, respectively. (d) An intensity profile taken along a line between the points X and Y in the TEM image (line width 50 pixels). (e,f) Enlarged intensity profiles from the gold and citrate regions, respectively.

conventional TEM image, atomic-resolution imaging is required to study these soft−hard interfaces.

An aberration-corrected transmission electron microscope (TEAM 0.5) operating at an accelerating voltage of 80 kV with a monochromated electron beam was used to obtain atomic-resolution images. A TEAM 0.5 image of a nanoparticle located near the edge of a graphene sheet is shown in Figure 3a. The hexagonal lattice of carbon atoms in the graphene support and the atomic columns in the cuboctahedral gold nanoparticle are easily seen. More importantly, the citrate coating and the citrate-gold interface are also clearly visible. To the best of our knowledge, this is the first direct atomic-resolution image of the surface molecules and interface on a nanoparticle.

The reflections of the gold nanoparticle and graphene sheet were identified through fast Fourier transformed (FFT) digital

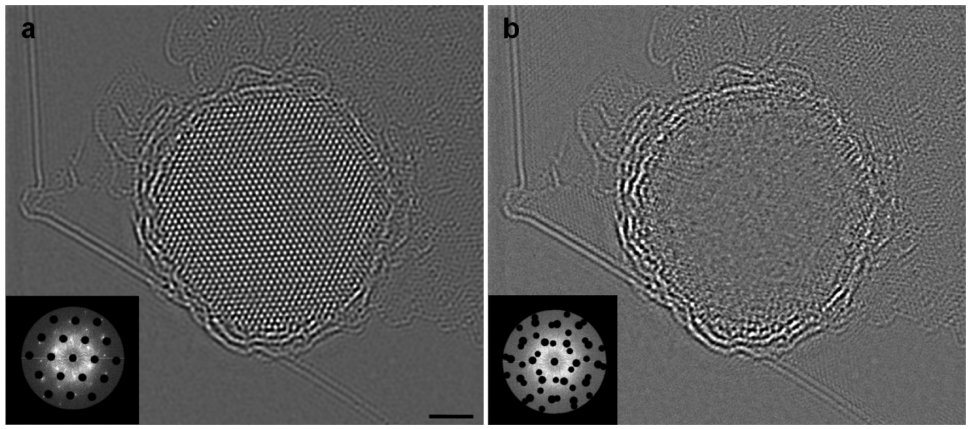

Figure 4. Graphene-enabled isolation and imaging of citrate molecules. (a) An enhanced-contrast filtered image of the citrate-capped gold nanoparticle. (Inset) The graphene reflections were subtracted in a digital diffractogram of the entire image. Scale bar represents 2 nm. (b) An image of the citrate molecules. (Inset) The graphene and gold reflections were masked in the digital diffractogram to isolate and image citrate.

Downloaded by U OF CALIFORNIA BERKELEY on September 22, 2009 | http://pubs.acs.org
Publication Date (Web): July 10, 2009 | doi: 10.1021/nl901664k

diffractograms obtained from different regions in the atomic-resolution image. An FFT of the graphene sheet, taken from the area indicated by the solid box in Figure 3a, exhibited hexagonal spot patterns that are characteristic of graphene (Figure 3b). Using the Miller−Bravais indices (hkil) for graphite, the inner hexagon corresponds to indices (1-110) and the outer hexagon corresponds to (1-210), which have lattice spacings of 2.13 and 1.23 Å, respectively. Hexagonal spots corresponding to both the gold nanoparticle and graphene support were clearly distinguishable in a digital diffractogram taken at the center of the nanoparticle, which is indicated by the dashed box. As shown in Figure 3c, the nanoparticle exhibited a strong reflection corresponding to 1/3{422} in reciprocal space, which has a 2.5 Å spacing, and the spots had characteristic relative angles of 60 .[19] Spots corresponding to [111] gold were also visible, such as the (220), (113), and (133) reflections, which have lattice spacings of 1.44, 1.23, and 0.93 Å, respectively. The rotation angle between the nanoparticle and graphene support was about 25 degrees obtained from the digital diffractogram of Figure 3a.

The atomic spacings in the gold nanoparticle and its surrounding citrate coating were determined through an intensity profile taken along a line connecting the points X and Y in Figure 3a. The profile corresponding to the nanoparticle revealed an average atomic spacing of 2.5 Å (Figure 3e), which confirms the FFT results. The citrate molecules on the nanoparticle were estimated to be 2−3 layers thick, and exhibited a spacing of 3.0−3.5 Å between layers (Figure 3f).

Invisibility of the graphene support was achieved by subtracting the periodic contrast of the carbon atoms in the graphene sheet in Fourier space. By masking the graphene reflections from a digital diffractogram of the entire imaged region (inset of Figure 4a), the atomic contrast of the graphene honeycomb lattice was removed and an enhanced-contrast filtered image of the gold nanoparticle and citrate molecules was obtained (Figure 4a). The atomic columns in the nanoparticle exhibited noticeable contrast variations in both the intensity profile (Figure 3e) and in the filtered image (Figure 4a), possibly due to nonuniformity in the citrate coating and interference with low atomic occupancy of columns at the nanoparticle perimeter. The crystalline structures of the graphene support and gold nanoparticle also enabled the isolated imaging of citrate. A filtered image of the citrate layers (Figure 4b) was obtained by removing both the graphene and gold reflections (inset of Figure 4b).

In conclusion, a graphene support enables direct imaging of organic molecules and interfaces with nanoparticles at a level previously unachievable. Such imaging capabilities can elucidate the properties of these surface layers and soft−hard interfaces, and provide scientists conducting theoretical studies with the experimental data for comparison. The atomic-resolution imaging demonstrated in this report can be used to directly observe nanoparticles functionalized with a diverse range of molecular coatings, such as DNA, proteins, and antibody/antigen pairs.[5] The detailed fine structure of the coating could be resolved by going to even lower microscope high-tensions and/or much lower temperatures, since the electron irradiation at 80 kV still results in specimen motion. We suggest that graphene can potentially become widely used in the TEM characterization of organic and inorganic nanomaterials.

Acknowledgment. This work was supported by the National Aeronautics and Space Administration and the National Center for Electron Microscopy, Lawrence Berkeley Lab, which is supported by the U.S. Department of Energy under Contract No. DE-AC02-05CH11231.

References

(1) Klajn, R.; Bishop, K. J. M.; Fialkowski, M.; Paszewski, M.; Campbell, C. J.; Gray, T. P.; Grzybowski, B. A. *Science* **2007**, *316*, 261.
(2) Tang, Z.; Zhang, Z.; Wang, Y.; Glotzer, S. C.; Kotov, N. A. *Science* **2006**, *314*, 274.
(3) Glotzer, S. C.; Solomon, M. J. *Nat. Mater.* **2007**, *6*, 557.
(4) Glotzer, S. C. *Science* **2004**, *306*, 419.
(5) Zhang, Z.; Glotzer, S. C. *Nano Lett.* **2004**, *4*, 1407.
(6) Shevchenko, E. V.; Talapin, D. V.; Kotov, N. A.; O'Brien, S.; Murray, C. B. *Nature* **2006**, *439*, 55.
(7) Nakata, K.; Hu, Y.; Uzun, O.; Bakr, O.; Stellacci, F. *Adv. Mater.* **2008**, *20*, 4294.
(8) DeVries, G. A.; Talley, F. R.; Carney, R. P.; Stellacci, F. *Adv. Mater.* **2008**, *20*, 4243.

(9) Khatri, O. P.; Adachi, K.; Murase, K.; Okazaki, K.; Torimoto, T.; Tanaka, N.; Kuwabata, S.; Sugimura, H. *Langmuir* **2008**, *24*, 7785.
(10) Khatri, O. P.; Murase, K.; Sugimura, H. *Langmuir* **2008**, *24*, 3787.
(11) Perepichka, D. F.; Rosei, F. *Angew. Chem., Int. Ed.* **2007**, *46*, 6006.
(12) Singh, C.; Ghorai, P. K.; Horsch, M. A.; Jackson, A. M.; Larson, R. G.; Stellacci, F.; Glotzer, S. C. *Phys. Rev. Lett.* **2007**, *99*, 226106.
(13) Neyman, A.; Meshi, L.; Zeiri, L.; Weinstock, I. A. *J. Am. Chem. Soc.* **2008**, *130*, 16480.
(14) Meyer, J. C.; Girit, C. O.; Crommie, M. F.; Zettl, A. *Nature* **2008**, *454*, 319.
(15) Meyer, J. C.; Kisielowski, C.; Erni, R.; Rossell, M. D.; Crommie, M. F.; Zettl, A. *Nano Lett.* **2008**, *8*, 3582.
(16) Balandin, A. A.; Ghosh, S.; Bao, W.; Calizo, I.; Teweldebrhan, D.; Miao, F.; Lau, C. N. *Nano Lett.* **2008**, *8*, 902.
(17) Frank, I. W.; Tanenbaum, D. M.; van der Zande, A. M.; McEuen, P. L. *J. Vac. Sci. Technol. B* **2007**, *25*, 2558.
(18) Dato, A.; Radmilovic, V.; Lee, Z.; Phillips, J.; Frenklach, M. *Nano Lett.* **2008**, *8*, 2012.
(19) Tsen, S.-C. Y.; Crozier, P. A.; Gajdardziska - Josifovska, M. *Microsc. Microanal.* **2002**, *8*, 1108.

NL901664K

Downloaded by U OF CALIFORNIA BERKELEY on September 22, 2009 | http://pubs.acs.org
Publication Date (Web): July 10, 2009 | doi: 10.1021/nl901664k